LIFT AND DRAG CHARACTERISTICS OF ROTATING OAR BLADES

By

William Durand Ramsey

SUBMITTED TO THE DEPARTMENT OF MECHANICAL

ENGINEERING IN PARTIAL FULFILLMENT OF THE

REQUIREMENTS FOR THE DEGREE OF

BACHELOR OF SCIENCE

at the

MASSACHUSETTS INSTITUTE OF TECHNOLOGY

May 7, 1993

© Massachusetts Institute of Technology

Signature of Author_____
Department of Mechanical Engineering
May 7, 1993

Certified by_____
Professor A. Douglas Carmichael
Thesis Supervisor

Accepted by_____
Professor Peter Griffeth
Chairman, Undergraduate Thesis Committee

1

LIFT AND DRAG CHARACTERISTICS OF ROTATING OAR BLADES

By

William Durand Ramsey

Submitted to the Department of Mechanical Engineering

on May 7, 1993 in partial fulfillment of the

requirements for the Degree of Bachelor of Science in

Mechanical Engineering

Abstract

This thesis examines the hydrodynamics of an oar stroke and presents lift and drag coefficients as functions of angle of attack. The goal of the thesis is to show the effect of rotational motion on the lift and drag characteristics of oar blades. A test rig simulates the motion of an oar blade by moving the blade in one direction while rotating it at constant angular speed. Sensors attached to the rig measure the dynamic forces on the blade. The oar blades were tested at four rotational speeds and two translational speeds . The data was collected and analyzed and the results show that lift and drag coefficients are greatly altered by rotating the oar blades at different frequencies.

Thesis Supervisor: Professor A. Douglas Carmichael

Title: Professor of Ocean Engineering

2

Table of Contents

List of Illustrations

Chapter 1   Introduction

Rowing has existed for thousands of years. Many ancient civilizations depended on the skill of their oarsmen for naval supremacy. While nations no longer depend on rowing for political standing, forums such as the Olympics preserve rowing as a symbol of international greatness. In as effort to advance the United States' Crew Team, in 1987 the United States Olympic Committee (USOC) awarded monetary grants to institutions to study rowing and develop more efficient techniques and equipment.

The USOC assigned MIT Sea Grant College Program the task of developing more efficient equipment for the crew team. The members of Sea Grant then decided to pursue the hydrodynamics of oar blades since any slight improvement in the efficiency of the oar blade would result in an increase in boat speed. This spawned a multi-year effort to understand the hydrodynamics of an oar stroke. Eventually this project came to be known as "The Oars Project."

Phil Wingard was sponsored to derive the state equations governing the dynamics of rowing and help generate a computer model. His Ocean Engineer thesis outlines the derivation of these state equations and gives an introductory understanding of the hydrodynamics of an oar stroke. The computer model calculated the forces on the oar at twenty points throughout a stroke. To do this a data set of lift and drag coefficients verses angle of attack was needed. Wingard assumed that the hydrodynamics of an oar stroke could be approximated as steady state and thus he set about obtaining static lift and drag coefficients. To do this he obtained half scale molds of existing oar blades from Concept II and then built a test rig to measure the forces on the model blades at various angles of attack. Wingard left MIT after finishing his thesis and never actually obtained these force coefficients. The computer model now in use was developed by Professor Carmichael.

Several students have continued with the Oars Project. In 1991, Chad Spooner and William Ramsey built an improved test rig to measure the forces on oar blades at constant angle of attack. Students in an Ocean Engineering Laboratory and Special Problems classes used this rig to test the oars and obtain lift and drag coefficients of the oar blades at ten degree increments of angle of attack from zero to 360 degrees. These results served as a useful first step in understanding the hydrodynamics of an oar stroke and as data points for use in the computer model.

As the computer model became more sophisticated, precise data was needed. The question arose as to what level of detail was needed in modeling the motion of an oar stroke and whether the static approximation was justified. Aerodynamic theory shows that rotating airfoils have different properties than static airfoils. In particular, stall is delayed on an airfoil undergoing a roll-up maneuver, as a result of delayed growth of the boundary layer. In a similar fashion, stall is accelerated on an airfoil decreasing its angle of attack as the boundary layer is unable to reattach itself to the airfoil. Taking these issues into account, it became necessary to include the dynamic motion of the blade when obtaining lift and drag coefficients.

This thesis presents simplified theory and analysis of the hydrodynamics of an oar stroke. The theory helps to model the stroke as the sum of a rotational velocity and a translational velocity and to explain various characteristics of the results obtained. A test rig was built to simulate the motion of an oar blade and measure the forces on the blade. Testing was conducted in the Ocean Engineering Towing Tank. Lift and drag coefficients verses angle of attack were obtained at a variety of Reynolds numbers and reduced frequencies. These results show the effects of reduced frequency on the lift and drag characteristics of oar blades.

Chapter Two Modeling an Oar Stroke

The motion of an oar blade is often linked to the motion of canoe or kayak paddles. These other devices are termed paddles and have the commonalty of deriving their propulsion by the production of drag. Most people think of oars as paddles because they neglect the motion of the boat when they picture an oar stroke. If the oar stroke were like that, drag would be the only propelling force. There have been several interesting and clever devices created which attempt to make use of this reasoning. One of these contraptions had a series of pulleys which enabled the oar blade to remain perpendicular to the boat throughout the entire stroke, the idea being to align all of the drag with the movement of the boat. Unfortunately for this innovative inventor oar blades differ from paddle devices in that much of the propulsion during an oar stroke is derived from lift, especially at the beginning and end of the stroke.

2.1 The Oar Blade as a Lifting Surface

Lift is defined as a force produced which is perpendicular to the free stream while drag is a force produced in line with the free stream. An easy example to illustrate this is an airfoil flying at an angle of attack with respect to the oncoming air. Lift is the force which counteracts gravity and enables the airplane to fly while drag is the force which slows the plane down and costs money to overcome.

This concept is slightly more difficult to picture when applied to oar blades. The lift and drag vectors are rotated into the plane of the water. The direction of the free stream defines the directions of lift and drag and is a function of boat speed, and angular position and angular velocity of the oar blade with respect to the boat. Another term for the free stream is the relative velocity, the velocity with which an observer on the oar blade witnesses the incoming water. The relative velocity is given by

$$\tilde{V}_{Rel;} = \tilde{V}_{Tan} + \tilde{V}_{Boat}$$

$$\tilde{V}_{Boat} = V_{Boat}\,\hat{e}_y$$

$$\tilde{V}_{Tan} = \omega r \cos\theta\,\hat{e}_x - \omega r \sin\theta\,\hat{e}_y$$

$$\tilde{V}_{Rel} = \omega r \cos\theta\,\hat{e}_x + (\,V_{Boat} - \omega r \sin\theta\,)\,\hat{e}_y$$

θ is the angle of the oar shaft with respect to the boat. ω is the angular velocity of the oar shaft and r is the radial distance to the oar blade from the oar lock. V_{Boat} is the instantaneous speed of the boat. The indices are defined by the direction of the boat. The y axis is in line with the boat velocity, while the x axis is perpendicular to the motion of the boat. The angle of the relative velocity and the oar blade is called the angle of attack, α, which is given by

$$\alpha = \tan^{-1}\left(\frac{\omega r \sin\theta + V_{Boat}}{\omega r \cos\theta}\right) - \theta$$

$$\alpha = \beta - \theta$$

These concepts are illustrated in Figure 1. Representative values of the relative velocity, angle of attack, angular position of the oar shaft, and boat speed are given in Table 1.

Table 1. Values of Relative Velocity and Angle of Attack for a Representative Oar Stroke

Oar Angle	Boat Speed	Attack Angle	Rel Velocity	Beta
45	4.1 m/sec	2	2.9	47
52.5	3.9 m/sec	10	2.4	62
60.9	3.6 m/sec	18	1.9	79
69.9	3.5 m/sec	30	1.5	99
79.7	3.5 m/sec	52	1.2	132
90.3	3.5 m/sec	92	1.1	182
101.2	3.7 m/sec	138	1.2	239
111.5	4.1 m/sec	169	1.6	280
120.8	4.5 m/sec	183	2.3	303
128.9	4.8 m/sec	189	3.1	319
135	5.0 m/sec	192	3.7	327

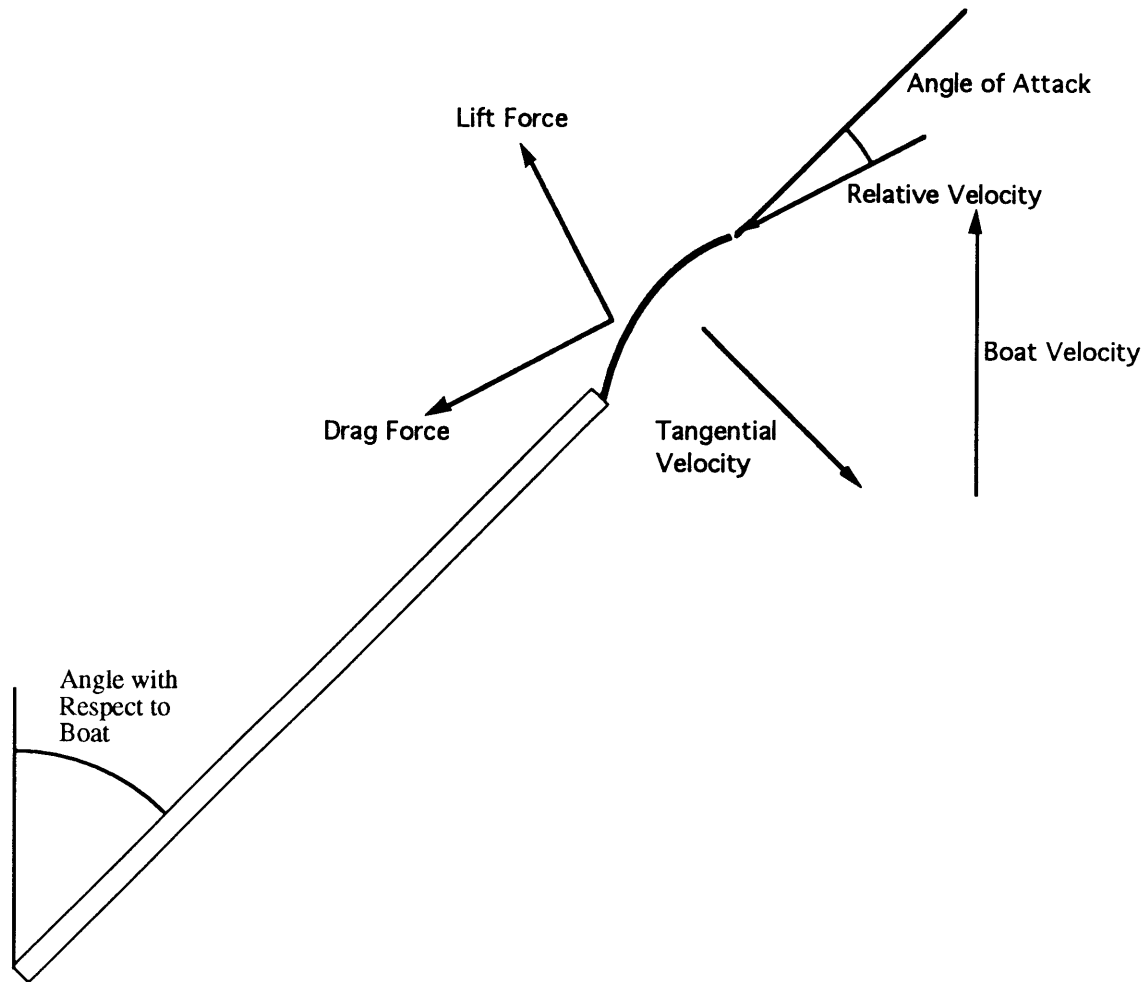Figure 1. The Oar as a Lifting Surface.

2.2 The Forces on the Oar

After determining the angle of attack and relative velocity throughout a stroke, the next step is to calculate the force on the blade. The force is divided into two components, lift and drag, which are given by

$$C_l = \frac{\text{Lift Force}}{\frac{1}{2}\rho V^2 A}$$

$$C_d = \frac{\text{Drag Force}}{\frac{1}{2}\rho V^2 A}$$

where A is the projected area of the oar blade and V is the magnitude of the relative velocity. C_l and C_d are functions of angle of attack and must be determined experimentally in a manner similar to obtaining force coefficients of airfoils in wind tunnels.

2.3 The Propulsive Efficiency

The column headed by β represents the angle of the relative velocity with respect to the boat. This parameter become important in the orientation of the forces and their effect on the propulsive efficiency during the stroke. The propulsive force of the oar blade is given by

$$F_{Propulsive} = \frac{1}{2}\rho V^2 A(C_l \sin \beta - C_d \cos \beta)$$

The force the rower feels is the force perpendicular to the oar shaft given by

$$F_{Perpendicular} = F_{Drag} \sin \alpha + F_{Lift} \cos \alpha$$

The efficiency, η, is defined as the ratio of the propulsive power of the oar to the power the rower exerts.

$$\eta = \left(\frac{P_{Propulsive}}{P_{Rower}}\right)_{Inst.} = \left(\frac{F_{Propulsive} V_{Boat}}{F_{Perpendincular} \omega r}\right)_{Inst.} = \left(\left(\frac{C_l \sin \beta - C_d \cos \beta}{C_d \sin \alpha + C_l \cos \alpha}\right)\frac{V_{Boat}}{\omega r}\right)_{Inst.}$$

For example, when $\beta = 180^o$, the relative velocity is aligned with the direction of the boat. This means that only the drag force propels the boat and lift has no effect on the speed of the boat. This happens during the middle of the stroke. When $\beta = 90^o$ or $\beta = 270^o$, the relative velocity is perpendicular to the boat meaning that lift is the force propelling the boat and that drag has no effect on the boat speed. While drag has no effect at these angles on the boat speed it should be noted that a component of drag is tangential to the oar blade and effectively wastes the oarsman's power. β becomes critical at the beginning and end of a stroke when β is less than 90° or greater than 270°. In these cases lift propels the boat as $\sin\beta$ which is less efficient. While this is cause for some concern, the major problem is that drag is oriented against the motion of the boat. Drag actually slows the boat down as $\cos\beta$. At the extremes of the stroke the lift to drag ratio becomes

10

very important as a measure of both the propulsive efficiency and the amount of rower's power wasted.

The efficiency, η, is a measure of the ratio of the rower's power applied to the water and the propulsive power moving the boat forward. As can be seen by the equation, the beginning and end of a stroke are excedingly inefficient, as much of the drag force actually impedes the boat's forward movement. One of the goals of the Oars Project is to increase the efficiency of the ends of the stroke by trying to understand the hydrodynamics of an oar stroke and then create a better oar blade.

Chapter Three Hydrodynamic Theory

The hydrodynamics of an oar stroke are extremely complicated and there are many areas to be considered in the analysis of a stroke. Several phenominon influence the macroscopic hydrodynamics of an oar blade such as the vorticy formation due to a low aspect ratio hydrofoil and the rotational effects. There are many other isuues such as the free surface and the role of turbulence which in order properly understand them would be the work of a PhD. thesis. In the foolowing sections brief hydrodynamic theory will be presented as an introduction to the basic hydrodynamics of an oar stroke.

3.1 Low-Aspect Ratio Airfoils

At the extreme ends of an oar stroke the oar blade acts similarly to a low aspect ratio airfoil airfoil, sometime referred to as a delta wing. The aspect ratio is a measure of the chord of a wing relative to its area given by

$$\text{Aspect ratio} = \frac{b^2}{S}$$

On an oar blade b=11", S= 39.97in^2,thus its aspect ratio is .28. Low aspect ratios have properties differing from infinite aspect ratio, or 2D, airfoils.

The most striking feature of delta wings is the formation of concentrated vortices running slightly aft of the leading edge. These vortices are produced by leading edge separation and subsequent reattachment. In potential flow the leading edge suction vector causes the drag to equal zero. On a delta wing the suction vector is rotated 90° and extra lift is produced. This extra lift component is termed vortex lift. Figure 2 shows the production of a vortex and figure 3 shows these vortices on a delta wing.

The generation of these vortices has a major effect on the lift characteristics of delta wings. The vortices prevent separation of the boundary layer and thus prevent stall. Delta wings can typically fly at angles of attack up to 45° before stall occurs. By comparison, 2D wings
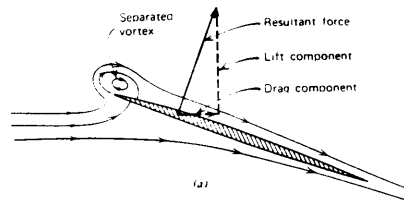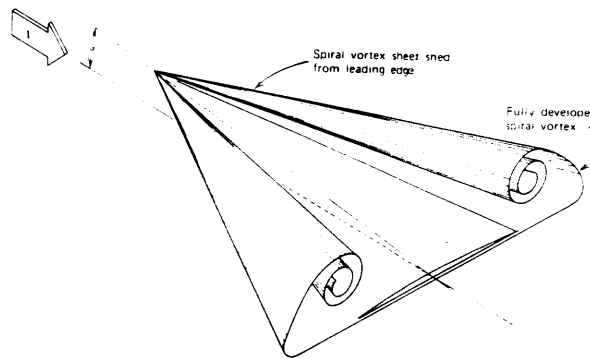
12

Figure 2. Leading Edge Vortex Formation[1]

Figure 3. Vortices on a Delta Wing[2]

normally stall around 15°. A drawback is that the lift curve slope for delta wings is greatly reduced and thus delta wings fly at higher angles of attack than 2D airfoils in order to produce enough lift.

Delta wings derive much of their lift from the production of these vortices. Lift is broken into potential lift and vortex lift. The total coefficient of lift is given by

$$C_l = \sin\alpha\cos\alpha(K_p\cos\alpha + K_v\sin\alpha)$$

The values of K_p and K_v are plotted against the aspect ratio in Figure 4.

---

[1] McCormick, Barnes W.. *Aerodynamics, Aeornautics, and Fight Mechanics.*
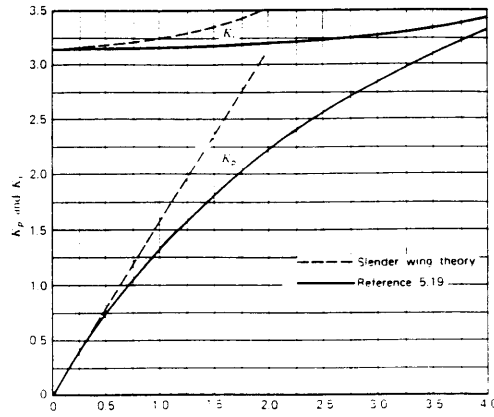[2] Ibid.

13

Figure 4. K_p and K_v as a Function of Aspect Ratio[3]

Experimental evidence on oar blades has indicated that these vortices may be important on delta shaped oar blades. The oar blade has been shown to be more efficient at the end of the stroke than at the beginning. This is because the vortices form over the surface of the oar blade and lower the pressure on the back side of the blade.

3.2 The Oar Blade as a Rotating Airfoil

The angles of attack of water relative to the oar blade range from approximately 2° to 192° during an oar stroke. Given that an oar stroke takes approximately one second, the rate of change of the angle of attack is $190^o/sec$. An oar stroke is very much a dynamic phenomenon and must be modeled as such.

The reduced frequency is a convenient way to incorporate rotational velocity, translational velocity, and size in one non-dimensional parameter, K, given by

$$\omega c/2u = K.$$

C is the chord length of the airfoil or oar blade. U is the free stream velocity. In aeroelasticity ω is the wings vibrational frequency. The equivalence of the wings flutter in an oar stroke would

---

3 Ibid.

be the sweep of the oar shaft. However, in this case the frequency of the angle of attack is being examined. Given this ω should equal 1.6 rad/sec, not .79 rad/sec. The discrepancy comes from the frame of reference. An observer riding on the oar blade oblivious to either the motion of the boat or the motion of the oar would perceive a change in angle of attack of 190°/sec, not 90°/sec. For this reason ω is taken from the change in angle of attack, not the change in oar angle.

3.3 Effect of Reduced Frequency on Lift and Drag

Properties of airfoils are governed by their reduced frequency. Just as bodies of revolution and airfoils have different properties dependent on their Reynolds number, they are affected by their rotational rate. At low frequencies, the airfoils approach steady state lift and drag values. At larger reduced frequencies, the properties of airfoils are dramatically changed. Stall is delayed on an airfoil increasing its angle of attack and, while its lift curve slope remains the same, higher lift coefficients are obtained. The opposite occurs with airfoils decreasing their angle of attack. The airfoil, presumably starting at an angle of attack greater than α_{stall}, will remain stalled and its lift coefficients are lowered greatly from their static values.

McCrosky in 1977 performed many experiments on NACA0012 airfoils at various reduced frequencies. McCrosky was analyzing the aerodynamics of an oscillating helicopter rotor blade. The results show dramatically the effect of reduced frequency of the lift and drag characteristics of airfoils. When the angle of attack is increasing stall is delayed and higher lift coefficients are obtained. However, when the angle of attack is decreasing the lift coefficients are a fraction of the static lift coefficients. In essence McCroskey's experiments are very similar to the ones in this thesis, the main difference being the medium and nature of the airfoil.

15

3.4 Boundary Layer Growth

Boundary layer growth of an airfoil is proportional to time. For laminer flow the equations of the boundary layer growth are

$$\frac{\delta}{c} = \sqrt{\frac{1}{Re}}$$

$$\delta = \sqrt{\nu t}$$

Thus the boundary layer of an impulsively started airfoil diffuses outward at a rate proportional to the square root of time. Stall is caused by an adverse pressure gradient within the boundary layer. An airfoil started from rest will not stall until it has moved several chord lengths because the boundary layer will not have grown enough to develop the adverse pressure gradient.

McCrosky's experiments show that stall is delayed on an airfoil increasing its angle of attack. This is due to the airfoil moving into the free stream faster that the boundary layer can develop. In some respects this is similar to a Mach cone produced by an airplane flying faster than the speed of sound. Since the boundary layer is unable to fully develop, an adverse pressure gradient is not produced until the airfoil is well over its stall angle. While the lift curve slope is unaltered, higher lift coefficients are obtained.

The increase of the lift curve slope may also be affected by vorticy shedding as the oar blade changes angle of attack. For every force that it generated in hydrodynamics a vortex must be shed of equal strength to the force. As the oar blade increases angle of attack and more lift is produced by the oar blade, vortices are shed proportional to the change in force such that

$$d\Gamma = \frac{dF}{\rho U}$$

. These vortices, like vortex inducers on commercial airplanes, serve to keep a turbulent boundary layer attached to the oar blade. In this manner the oar blade can produce more lift.

A similar line of reasoning holds for an airfoil decreasing its angle of attack. The airfoil is presumably already stalled as it begins to decrease its angle of attack. The boundary layer will

be unable to reattach itself to the airfoil because the surface of the airfoil is moving faster than the boundary layer can develop. In this case the airfoil will not produce much lift until the angle of attack is well below the angle of stall of a static airfoil and the pressure gradient is favorable enough to cause the flow to reattach itself.

3.5   The Oar Blade as a Symmetrical Airfoil

The oar blade unlike most airfoils operates with angles of attack from approximately 0° to 190°. Zero lift occurs at angles of attack of about 10° and 190°. Hence, when the angle of attack is 165°, the absolute angle of attack, defined as the angle with respect to zero lift, is 25°. The absolute angle of attack is important when analyzing the effect of rotation at the beginning and end of an oar stroke. At the beginning of an oar stroke the absolute angle of attack is increasing; the angle of attack is increasing from zero lift towards the stall angle. At the end of the stroke the angle of attack is still increasing, but the absolute angle of attack is decreasing.

From the data on reduced frequency already presented some effects of the rotational motion on the hydrodynamics of an oar blade can be estimated. At the beginning of the stroke when the absolute angle of attack is increasing stall is expected to be delayed and higher lift coefficients should be obtained. Likewise at the end of the stoke the oar blade should remain stalled and lower lift coefficients should be obtained.

3.6 Other Effects

Many of the dominating factors of the hydrodynamics of an oar stroke have been presented. There still remain several areas which cannot be analyzed at the present time.

The first and most significant effect is the free surface. An oar blade is placed in the water such that its upper surface is approximately even with the water. Relating this to an airfoil it is as if the side edge of a wing were bounded by a free surface. While an infinite wing may be

17

little affected by this, a delta wing obtaining much of its lift from the production of vortices may be greatly affected by the role of the free surface in the formation of vortices.

The second major issue is turbulence. Much of the oar stroke is turbulent. When the oar is initially placed in the water turbulence is created. At the middle of the stroke the flow is entirely separated and remains turbulent throughout the rest of the stroke. The effect of turbulence cannot and will not be discussed further in this thesis.

Chapter 4 Test Apparatus

The experiments were conducted in the Ocean Engineering Towing Tank. A carriage runs down the length of the tank at speeds controlled by a drive system. A force transducer was attached to the carriage. A servomechanism mounted to the force transducer rotates the oars at a constant angular velocity. Figure 5 shows the set up.
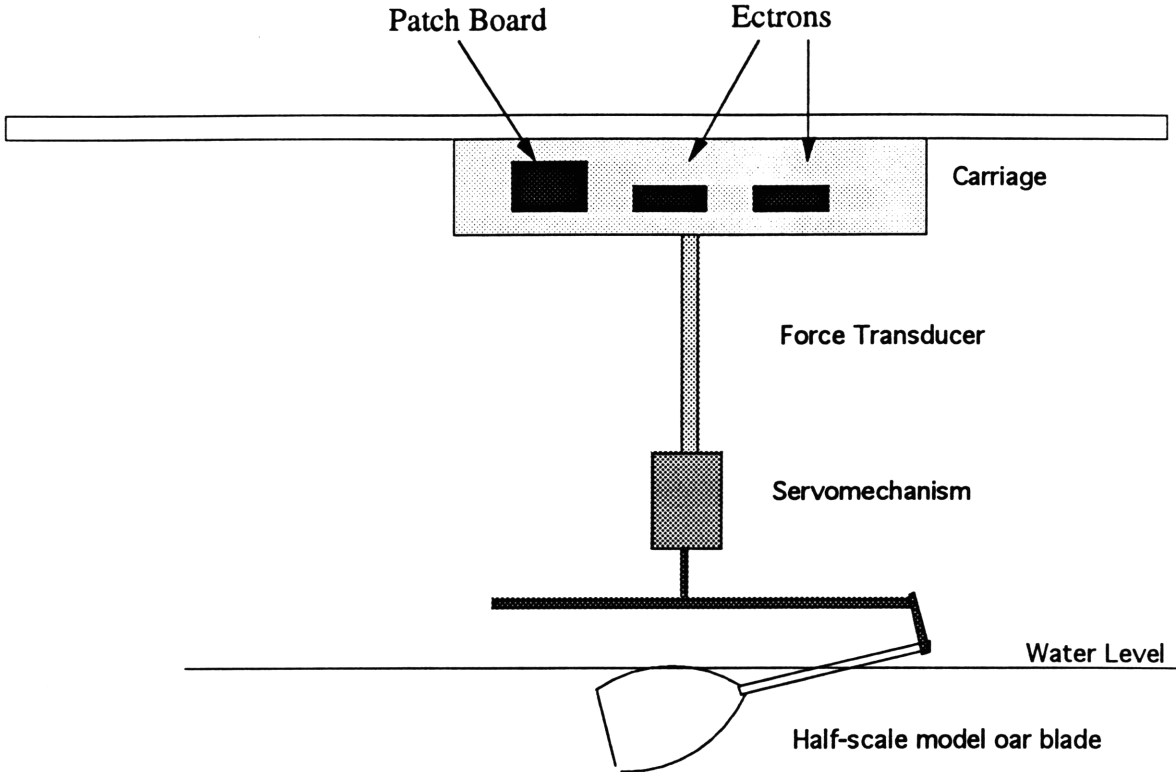
Figure 5. Experimental Set up in the Towing Tank

4.1 Force Transducer

The force transducer converts the dynamic force on the oar to a voltage which can then be analyzed to determine the forces on the oar. The transducer was constructed from

a 1.5" diameter aluminum round stock. At two locations 0.8875 ft. apart the stock was turned to 1 in. external diameter and 0.825 in. internal diameter achieving a 0.125 in. wall thickness at a radius of 0.5 in.. The purpose of the decreased wall thickness was to increase the stress level at the two locations and serve as a decent location for the placement of strain gauges. The maximum stress a five pound force on the oar blade would yield was calculated to be 5000psi., an acceptable percentage of the yield stress of aluminum.

The round stock was welded to a square aluminum plate on one end and a circular plate on the other. The circular plate was indexed to serve as a means of setting the angle of attack for static testing. The square plate provided a reference axis for the placement of strain gauges and a means to align the transducer with the carriage motion. Four mean lines were marked on the round stock corresponding to each side of the square. Strain gauges were then mounted such that each strain gauge straddled the mean line. The strain gauges used differed from typical strain gauges in that each gauge contained two resistors side by side. The strain gauges were wired into four Wheatstone circuits, two measured lift moments and two measured drag moments. In a typical Wheatstone circuit only two of the resistors are active strain gauges. The advantage of the strain gauges is that all four of the resistors are active strain gauges of the same resistance thereby increasing the gain and resolution of the signal produced.

The Wheatstone circuit was amplified and balanced using Ectron amplifiers. The four signals were then connected to a patch board and run into a computer which recorded the data. Figure 6 shows the circuitry of the strain gauges.

4.2 Servomechanism

Many factors had to be considered for the design of a mechanism to rotate the model oar blades at a constant angular velocity: ease of operation, reliability, adaptability
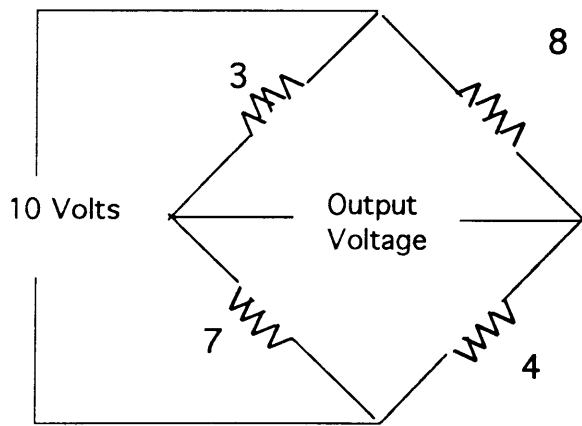
to the existing force transducer, and cost. The main options were digital feedback systems, step motors, and servo systems. A servo system was chosen because it best satisfied the design criteria. Once the type of control system was decided upon the next step was to design the actual servomechanism to rotate the blades. Two main functional requirements dominated this phase: stiffness to prevent vibration and concentricity to align the oar blade with the axis of the force transducer.
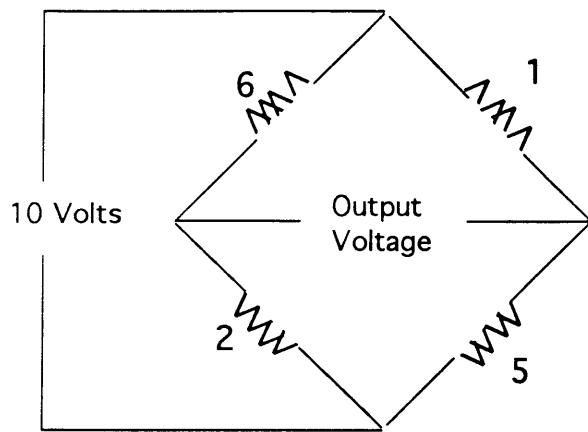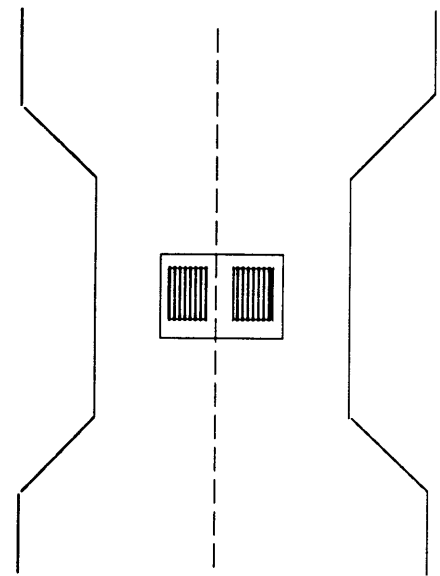
Lift Wheatstone Bridge

Drag Wheatstone Bridge
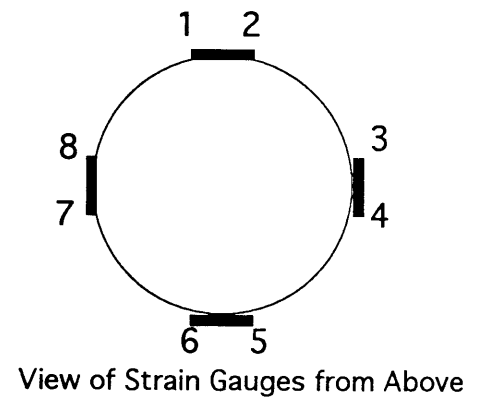
View of Strain Gauges from Above

Side View of Strain Gauges

Figure 6. Placement and Wiring of Strain Gauges.

A circular piece of aluminum stock was turned on the inside and outside. The circular piece served as both a structural housing for the unit and as a basis for the concentricity of the structure. Three half inch aluminum plates were then turned to fit tightly inside the housing such that their centers aligned precisely. Two of the plates held NSK bearings and the third secured a Helipot 20K infinite turn potentiometer. The potentiometer served as a means to determine angle of attack. Its resistance ranged from zero to 20K during one revolution and thus every angular position corresponded to a unique resistance. This point is important in that the potentiometer was coupled to the shaft which rotated the oar blade and was used to determine the angle of attack of the oar blade. The drive shaft was .75" in diameter and was located in the center of the structure. A no-slip belt system connected the shaft, motor, and tachometer. Three revolutions of the motor rotated the shaft once and the tachometer shaft six times.

The output from the tachometer and the input to the motor were connected to an MC-5 mounting card. The mounting card matched a specified command voltage to the tachometer voltage by adjusting the motor's voltage and in this way maintained a constant rotational rate despite any torques on the shaft. The power to the mounting card was provided by a Zytek 24V 6A power supply. Figure 7 shows the servomechanism.
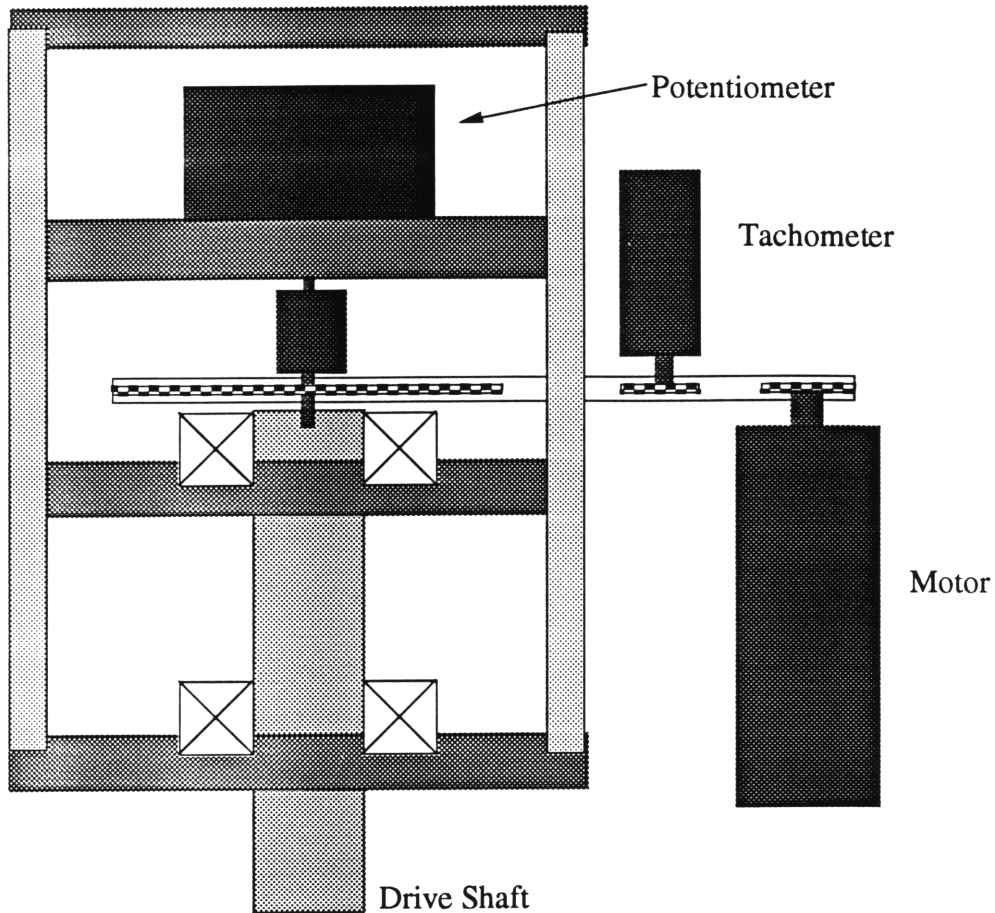
Figure 7. Servomechanism

4.3 Half Size Oar Blades and Blade Attachment

The half scale oar blades were constructed by laying fiberglass in a mold obtained from Concept II. A numerically controlled milling machine used a modified program to mill out the complex three dimensional shape of a half scale oar blade. The oar shaft was made from a half inch diameter aluminum tube.

The oar shaft was bolted to a square aluminum rod connected to the drive shaft of the servomechanism. The rod fits exactly into a slotted groove in the drive shaft and is bolted into place. This allows precise positioning of the oar. The torques produced by

the weight of the oar and attachment are easily canceled by placing weights on the rod. This is to insure a consistent zero value of the strain gauges as the oar revolves.

Chapter 5 Testing

5.1 Translational and Rotational Speed

The oar blades were tested at two Reynolds numbers and four rotational speeds. Since the chord length of a full size oar blade is twice the chord length of the half scale blade and its average relative velocity is 2 m/sec, the half scale oar blade should have been tested at a velocity of 4 m/sec in order to maintain a constant Reynolds number. The carriage in the Towing Tank was limited to speeds of 1.25 m/sec due to excessive vibration in the system. This presented a problem, since the Reynolds number of the model oar blades was less than a quarter of the Reynolds number of the full size oar blades. The model oars were tested at two different translational speeds to show that the lift and drag coefficients remained constant independent of their Reynolds number and thus could still be applied to a higher Reynolds number oar blade.

After determining the appropriate translational velocity of the model oar blade, the next parameter to determine was the rotational rate of the oar blade. The reduced frequency parameter was used to scale the ratio of the angular velocity and the translational velocity of airfoils of varying sizes and rotation rates. As with the Reynolds number, there are different "regimes" of reduced frequencies for which the properties of airfoils are different. On a full size oar blade ω=3.31 rad/sec, U=2 m/sec, c=.5m, so K=.41. In order to maintain a constant reduced frequency on a half size oar blade moving at .25 m/sec, ω should be .8275 rad/sec. As the translational velocity increases, ω must increase as well.

5.2 Setting the Blade in the Water

The oar blade was placed in the water such that the shaft was inclined 14° relative to the surface of the water to match the angle an actual oar shaft makes relative to the water. The "pitch" defines the angle the blade makes with respect to the shaft. On a full size blade the pitch is normally 5°, but in the testing the pitch was neglected. The blade was placed just deep enough in the water so that the top surface of the blade was flush with the surface of the water.

5.3 Data Collection

The outputs from the Ectron amplifiers and the potentiometer were connected into a patch board located on the carriage. Form the carriage the signals were run into the control room where they were fed into a computer. The computer recorded the data using the program STREAMER. The signal was sampled at 1 KHz for 75 seconds. The length of the sample time enabled several sets of data to be obtained from one run of the carriage. The data was converted to matrix format suitable for use with MATLAB by a program written by Dave Barrett.

5.4 Calibration

The strain gauges and potentiometer required calibration to determine their zero values, moment/voltage constant for the strain gauges, and angular position as a function of potentiometer voltage. A one pound force was applied to a balanced shaft at a distance of 1', thus applying a 1 ft lbs. moment to the force transducer. The servomechanism rotated the moment through several revolutions thus applying a moment of $(sin\alpha)$ 2ft lbs.

to both drag channels and $(\cos \alpha)2$ ft lbs. to both lift channels. The moment/voltage

constants were obtained by measuring the amplitudes of the curves.

$$C_{Calibration} = \frac{Voltage_{max} - Voltage_{min}}{2 \text{ ftlbs.}}$$

The zero value was calculated in a similar fashion.

$$Z = \frac{Voltage_{max} + Voltage_{min}}{2}$$

The potentiometer was calibrated by comparing its voltages corresponding the locations

of the peaks and zero values of the sine curves and realizing that the angular position of

these should be multiples of 90°. The equation produced for the potentiometer to yield

the angle of attack is

$$\alpha = \frac{Voltage_{Pot.}}{.0298} - 91.9631$$

The strain gauge constants and zero values are listed in Table 2.

Table 2. Strain Gauge Constants.

Channel	M/V Constant	Zero Value
Drag 1	0.9761	-0.5769
Drag 2	0.9797	-0.5795
Lift 1	0.6579	-0.0926
Lift 2	1.8772	-0.0603

Chapter 6 Results

Five channels of raw data were converted into a matrix which was five columns by 7400 rows. Using MATLAB these were reduced into lift and drag coefficients. The magnitude of the force on the blade is related to the moments measured by the force transducer at two different locations by

$$F_{Hydrodynamic} = \frac{M_2 - M_1}{L_1}$$

M_1 and M_2 are the moments measured by the upper and lower strain gauges respectively. L_1 is distance between the strain gauges and is 0.8875 ft.. Using this equation, the coefficient of force is given by:

$$C_f = \frac{(Voltage_2 - Z_2)C_2 - (Voltage_1 - Z_1)C_1}{L_1\left(\frac{1}{2}\rho V^2 A\right)}$$

The position of the force was obtained from:

$$X_f = \frac{(Voltage_1 - Z_1)C_1 L_1}{(Voltage_2 - Z_2)C_2 - (Voltage_1 - Z_1)C_1}$$

For some unknown reason, the drag channels recorded almost exactly the same data. Drag coefficients were obtained by assuming the position of force was located at L_1 + X_f. Using that value, the force was calculated from the moments measured. The values for drag are not acurate, but are useful in showing the trend of reduced frequency on drag. The lift and drag coefficients were then plotted against angle of attack at speeds of either .5 knots or 1 knot. The data presented in this section shows this lift and drag coefficients at rotational rates of 4 RPM, 9 RPM, 13.5 RPM and 17 RPM on each graph.
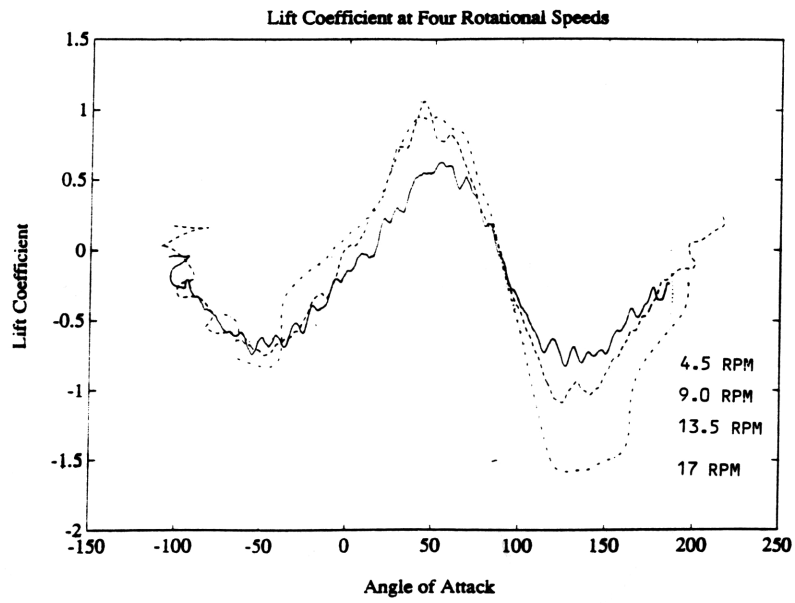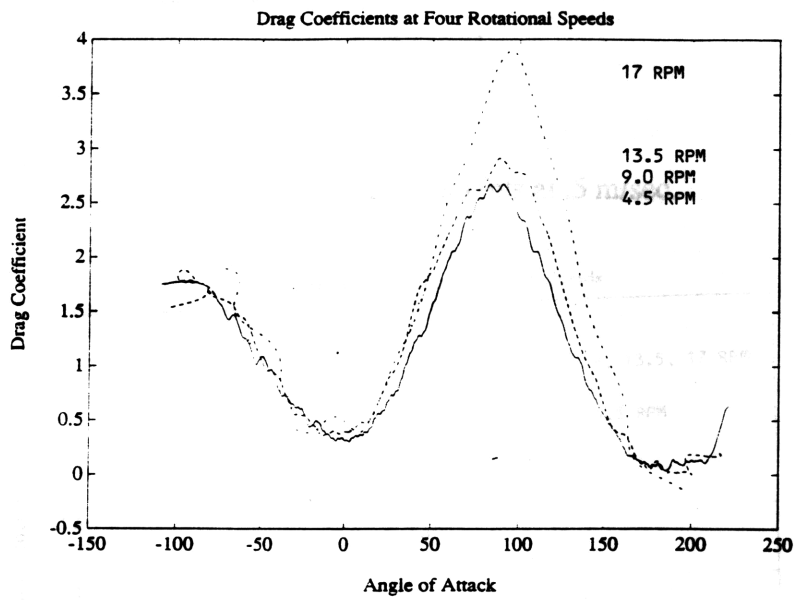
28

Figure 8. Lift Coefficients at .25 m/sec
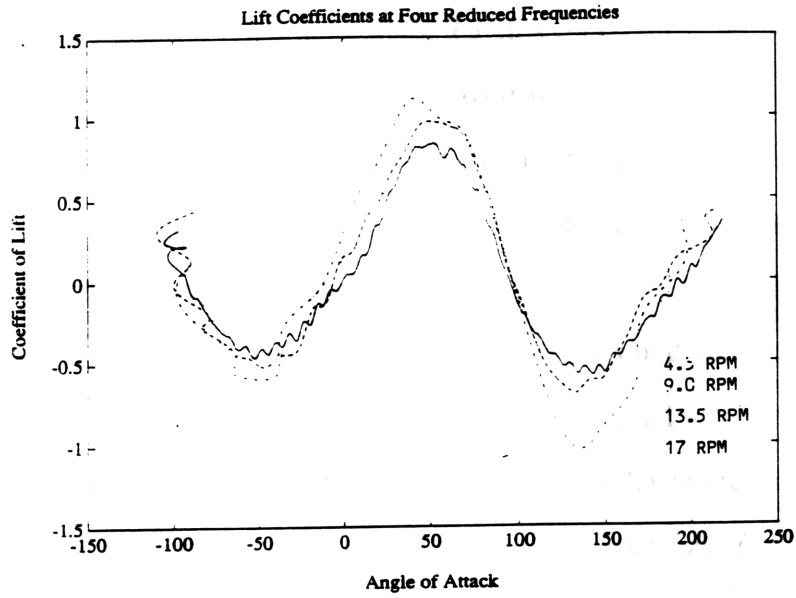

Figure 9. Drag Coefficients at .25 m/sec

Lift Coefficients at Four Reduced Frequencies

Figure 10. Lift Coefficients at .5 m/sec.
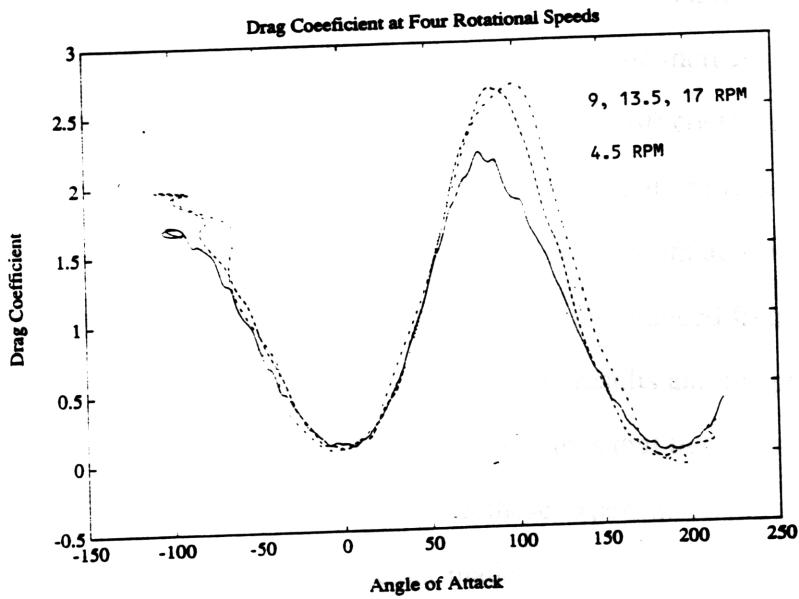
Drag Coeeficient at Four Rotational Speeds

Figure 11. Drag Coefficients at .5 m/sec.

30

Chapter 7 Analysis of Results

The results show many interesting features concerning the hydrodynamics of oar blades. A brief glimpse at Figures 6-9 reveals that rotating oar blades have much different lift and drag characteristics than static oar blades. A more in depth examination of the results leads to some conclusions which match predictions based on McCroskey's research and others which do not.

The first important result is the increase in lift around 45°. It was hypothesized that the lift curve slope would remain unaltered but that stall would be delayed, so that higher lift coefficients could be attained at increased angles of attack. The results show a dramatic increase in lift which is to be expected. However, the lift curve slope increases with rotation, and stall occurs at the same angle of attack irrespective of rotation.

The second major result is the change in lift from 135° to 180°, corresponding to the end an oar stroke. The lift coefficients should be lowered because of turbulence and the unfavorability of reattaching the boundary layer. The data does not confirm this theory. Instead, Figures 8 and 10 show a clear and dramatic increase in lift coefficients as the reduced frequency increases. In fact the maximum lift coefficient of the oar at 17 RPM is nearly twice as large as the maximum lift coefficient of the oar at 4 RPM. As with the lower angles of attack, the stall angle remains constant at around 135° for all rotational rates and the lift curve slope increases with the reduced frequency.

A possible reason for the discrepancy of these results and the predictions has to do with the location of the pivot point. The theory assumes that the pivot point is located at the trailing edge of the oar blade. However, in these experiments the oar blade was pivoted about the mid-chord. When the oar blade is increasing its absolute angle of attack at the beginning of a stroke the leading edge is moving into the flow while the trailing edge is moving away from the flow. This would account for why the lift

31

coefficients produced by the increased rotation rate were not as much larger than the static case as would have been expected.

At the end of the stroke the hydrodynamics become more complicated. The oar blade is completely turbulent, as evidence shows from the increase in drag coefficients at an angle of attack of 90°. In order to produce lift the boundary layer must be reattached to the surface of the oar blade In general, separation first occurs on the trailing edge of airfoils. Thus, a stalled airfoil will produce more lift if the flow would reattach to the trailing edge. By having the pivot point in the middle of the oar blade, at the end of the stroke the trailing edge is moving into the turbulence. This would help create a favorable pressure gradient and would help the flow reattach and produce lift. This hypothesis is confirmed from the data.

Another interesting topic is the effect of reduced frequency on drag. Figures 9 and 11 show a symmetrical distribution of drag about 90° angle of attack. This would be expected because at 90° the oar blade is perpendicular to the free stream. The drag dramatically rises at 90° as the reduced frequency increases due to more turbulence being produced. The drag does not change considerably at either low or high angles of attack according to the data.

Chapter 8 Conclusions

The purpose of this paper was to produce lift and drag coefficients of oar blades and show the effect of rotational rate on the lift and drag characteristics of oar blades. The data presented is this paper conclusively shows that rotational rate greatly affects the lift and drag at three main locations during the stroke.

At the beginning of the stroke when the angle of attack is less than 45°, the lift coefficients are larger when the rotation rate is higher. Likewise, at the end of the stroke when the angle of attack is greater than 135°, the lift coefficients are increased considerably as well. During the middle of the stroke the angle of attack is 90° and drag is the only propelling force. At angles of attack of 90° the drag coefficients are also increased as the rotational rate goes up. Thus it can easily be seen that increasing the rotational rate of the oar blade improves the efficiency of an oar stroke.

The significance of this paper is that it demonstrates that the rate of change of the angle of attack must be taken into account when choosing a data set of lift and drag coefficients for use in the computer simulation of an oar stroke. The results also show that the static approximation is not justified.

Bibliography

Chow, Chuen-Yen and Kuethe, Arnold M. *Foundations of Aerodynamics*. John Wiley and Sons, New York. 1986.

McCroskey, W.J. *Dynamic Stall Experiments on a NACA 0012 Airfoil*. NASA TP1100, 1977.

McCormick, Barnes W.. *Aerodynamics, Aeronautics, and Flight Mechanics*. John Wiley and Sons, New York. 1979.